Carthamus tinctorius L. inhibits hepatic fibrosis and hepatic stellate cell activation by targeting the PI3K/Akt/mTOR pathway

ZHIHENG DONG[1*], HAIBIN GUAN[2*], LU WANG[3], LIJUAN LIANG[2], YIFAN ZANG[2], LAN WU[4] and LIDAO BAO[5]

[1]Department of Pharmacy, Affiliated Hospital of Inner Mongolia Medical University, Hohhot, Inner Mongolia Autonomous Region 010030, P.R. China; [2]College of Pharmacy, Inner Mongolia Medical University, Hohhot, Inner Mongolia Autonomous Region 010110, P.R. China; [3]College of Basic Medicine, Inner Mongolia Medical University, Hohhot, Inner Mongolia Autonomous Region 010110, P.R. China; [4]Mongolia Medical School, Inner Mongolia Medical University, Hohhot, Inner Mongolia Autonomous Region 010110, P.R. China; [5]Department of Pharmacy, Hohhot First Hospital, Hohhot, Inner Mongolia Autonomous Region 010030, P.R. China

Received March 20, 2024; Accepted July 19, 2024

DOI: 10.3892/mmr.2024.13314

Abstract. Hepatic fibrosis (HF) is a process that occurs during the progression of several chronic liver diseases, for which there is a lack of effective treatment options. *Carthamus tinctorius L.* (CTL) is often used in Chinese or Mongolian medicine to treat liver diseases. However, its mechanism of action remains unclear. In the present study, CTL was used to treat rats with CCl_4-induced HF. The histopathological, biochemical and HF markers of the livers of the rats were analyzed, and CTL-infused serum was used to treat hepatic stellate cells (HSCs) in order to detect the relevant markers of HSC activation. Protein expression pathways were detected both *in vitro* and *in vivo*. Histopathological results showed that CTL significantly improved CCl_4-induced liver injury, reduced aspartate aminotransferase and alanine aminotransferase levels, promoted E-cadherin expression, and decreased α-smooth muscle actin (SMA), SOX9, collagen I and hydroxyproline expression. Moreover, CTL-infused serum was found to decrease α-SMA and collagen I expression in HSCs. Further studies showed that CTL inhibited the activity of the PI3K/Akt/mTOR pathway in the rat livers. Following the administration of the PI3K agonist 740Y-P to HSCs, the inhibitory effect of CTL on the PI3K/Akt//mTOR pathway was blocked. These results suggested that CTL can inhibit HF and HSC activation by inhibiting the PI3K/Akt/mTOR pathway.

Correspondence to: Professor Lidao Bao, Department of Pharmacy, Hohhot First Hospital, 150 South Second Ring Road, Hohhot, Inner Mongolia Autonomous Region 010030, P.R. China
E-mail: 320795027@qq.com

Professor Lan Wu, Mongolia Medical School, Inner Mongolia Medical University, 5 Xinhua Street, Hohhot, Inner Mongolia Autonomous Region 010110, P.R. China
E-mail: xbnz07091112@163.com

*Contributed equally

Key words: hepatic fibrosis, *Carthamus tinctorius L.*, hepatic stellate cell, PI3K/Akt/mTOR pathway

Introduction

Hepatic fibrosis (HF) is a pathological process in which the liver performs damage repair responses to various chronic stimuli such as chronic viral infection, alcohol consumption, parasitic disease, genetic abnormalities and toxic damage (1,2). Extracellular matrix (ECM) components, mainly collagen, deposited in the liver cause contracted scarring and increased organ stiffness (3). Hepatic stellate cells (HSCs) represent the most important inducers of fibrosis following liver injury. Under the action of various cytokines such as tumor necrosis factor α, interleukin-1β, interleukin-6 and transforming growth factor-β1 (TGF-β1), HSCs are continuously converted into fibroblasts, producing large amounts of ECM components that eventually cause HF (4,5). HSC proliferation, cell phenotype transformation, and increased synthesis of ECM and deposition, combined with neovascularization and inflammation, represent the most prominent pathological features in the repair and reconstruction of progressive HF (6,7).

A significant body of evidence has shown that signaling pathways play an important role in HF, particularly the PI3K/Akt/mTOR pathway, which is particularly important during inflammation and apoptosis (8,9). Previous studies have found that in carbon tetrachloride (CCl_4)-induced animal models of HF and HSC activation, the PI3K/Akt/mTOR pathway is activated and that inhibition of this activation could reduce the production of ECM, thereby inhibiting HF and HSC activation (10-13). Wang *et al* (14) found that salvianolic acid A attenuates CCl_4-induced HF by regulating the PI3K/AKT/mTOR signaling pathways. Similarly, interleukin-22 has been found to alleviate alcohol-associated HF by inhibiting the PI3K/AKT/mTOR pathway (12). Germacrone also improves HF by regulating the PI3K/AKT/mTOR signaling pathway (15). Therefore, the PI3K/AKT/mTOR pathway is particularly important for HF.

Carthamus tinctorius L. (CTL) is a cash crop with multiple functions. The flowers and seeds of CTL are traditional herbs that have a range of applications in China, Korea, Japan, and

other Asian countries (16,17). CTL has been used to treat gynecological, cardiovascular, and cerebrovascular diseases (18,19). Numerous substances, including flavonoids and alkaloids, have been isolated and identified from CTL (20). Water-based CTL extracts, such as hydroxysafflor yellow A, have been developed as injections to treat cardiovascular disease in China (21), and extracts of CTL seeds have been used to treat osteoporosis in Korea (16). Numerous clinical and experimental studies have focused on the therapeutic effects of CTL, with some results indicating that CTL has potential clinical value (22-24). However, research into the mechanisms of CTL action is scarce. By reviewing several studies, it was found that numerous traditional Chinese and Mongolian remedies that are used to treat liver disease contain CTL as the main active ingredient (25-28). However, its mechanism of action remains unclear.

In the present study, to clarify the mechanism of action of CTL for the treatment of HF, CTL was used as an intervention in a rat model of HF and pathological liver changes and ECM liver tissue contents were assessed. Serum infused with CTL was also used to treat activated HSC cells to detect the biomarkers present in the activated cells and characterize the activity of the PI3K/AKT/mTOR signaling pathway in both the animals and cells. The results of the present study suggest that CTL has the potential to inhibit PI3K and has the potential to be further developed as a therapeutic drug for HF.

Materials and methods

Animals and treatments. A total of 40 male Sprague-Dawley rats (age, 6-weeks-old; weight, ~200 g) were purchased from Inner Mongolia Medical University. All experiments were conducted according to The Guidelines for the Use and Maintenance of Experimental Animals in China and were approved by The Ethics Committee of Inner Mongolia Medical University (Hohhot, China; approval no. YKD202201124). The animals were acclimatized for one week, with conditions at a controlled temperature of 22±2˚C and a humidity level of 50±10% in the designated facility, allowed unrestricted access to food and water, and acclimated to alternating 12-h light and dark cycles. Animals were subsequently divided into five groups (n=8/group). The HF model rats were given intraperitoneal injections of 50% CCl_4 in olive oil twice per week for 8 consecutive weeks, while the control rats were given the same dose of pure olive oil over the same period. To prepare the drug, ultrafine powder was used for the extraction of CTL. A total of three methods for the extraction of herbal compounds were compared: i) Ultrasonic extraction, in which CTL ultrafine powder was dissolved in 5% sodium carboxymethylcellulose and extracted by ultrasonic treatment at 60˚C for 1 h; ii) ethanol extraction, in which CTL ultrafine powder was dissolved in 75% ethanol and extracted for 24 h; and iii) heat reflux extraction, in which CTL ultrafine powder was refluxed in boiling water and extracted for 2 h (a traditional herbal extraction method). Using mass spectrometry methods were used for detection. Briefly, mass spectrometry analysis was performed using a Thermo Orbitrap Exploris 120 mass spectrometer (Thermo Fisher Scientific, Inc.) equipped with an electrospray ionization source operating in positive and negative ionization modes. The following parameters were utilized: Positive ion spray voltage at 3.50 kV; negative ion spray voltage at -2.50 kV; sheath gas flow rate at 11 l/min with 350˚C; drying gas flow rate at 8 l/min with 320˚C; nebulizer pressure at 40 psi; full scan mass spectrometry analysis was conducted at a resolution of 60,000 FWHM (full width at half maximum) over the m/z range of 100-1,000. The three methods yielded almost the same extracts. However, in terms of extraction efficiency, ultrasonic extraction at 60˚C was similar to ethanol extraction, but both these methods had greater efficiency than boiling water extraction (data not shown). Finally, the ultrasonic extraction method was selected for the subsequent experiments.

After 4 weeks of CCl_4 treatment, three groups were selected and treated with CTL. For dosage selection, the dosages used in another study were referred to (29), and preliminary studies with CTL dosages of 0.1, 0.5, 1.5, 4.5, 7.5 and 15 g/kg gavage were performed. A dose of 0.1 g/kg exhibited minimal pharmacological activity, whereas comparison doses of 7.5-4.5 g/kg did not indicate enhanced pharmacological efficacy (data not shown). Ultimately, to demonstrate the dose-dependent effect of CTL, three CTL dosages, 0.5, 1.5 and 4.5 g/kg, were selected and administered for 4 weeks. Accordingly, the five experimental groups were as follows: i) Control group; ii) Model group; iii) CTL low-dose group (CTL-L; 0.5 g/kg); iv) CTL medium-dose group (CTL-M; 1.5 g/kg); and v) CTL high-dose group (CTL-H; 4.5 g/kg). The rats were euthanized by placing them in a sealed container filled with CO_2 (volume displacement rate, 70% vol/min). Blood was collected from the abdominal aorta, and centrifuged at 3,000 x g and 4˚C for 15 min to collect serum using a gel/coagulant tube, and finally stored at -80˚C. The right lobe of the liver was then excised, fixed in a 4% paraformaldehyde solution at room temperature for 24 h, while the remaining liver tissue was preserved in liquid nitrogen.

HSC culture and treatment. Primary HSCs were isolated from the livers of the rats according to a previously described protocol (10). Rat HSC-T6 cells (Pricella; cat. no. CL-0116) were thawed and revived according to the manufacturer's instructions. All cells were cultured in a 5% CO_2 atmosphere at 37˚C in Dulbecco modified Eagle medium (DMEM) (Thermo Fisher Scientific, Inc.) supplemented with 10% fetal bovine serum (FBS) (Gibco; Thermo Fisher Scientific, Inc.), 100 U/ml penicillin and 100 U/ml streptomycin (Thermo Fisher Scientific, Inc.). Primary HSCs were activated by culturing on plastic cell culture flasks at 37˚C for 7 days. The HSC-T6 cells were then treated with 10 ng/ml TGF-β1 (Sigma-Aldrich; Merck KGaA) at 37˚C for 24 h to activate them.

For preparing CTL-infused serum, the rats were administered CTL at doses of 0.5 g/kg (CTL-L), 1.5 g/kg (CTL-M) and 4.5 g/kg (CTL-H) for 5 days. The rats were fasted on the final day, and blood samples were collected using the abdominal aorta method in a separation gel/coagulant tube 3 h after the last gavage (30). The sample was centrifuged at 3,000 x g at 4˚C for 15 min to separate the serum, followed by sterilization with a microporous filtration membrane. To investigate the effects of CTL on the activation of primary HSCs, CTL-infused serum samples from the three groups (CTL-L, CTL-M and CTL-H) at a concentration of 10% of the culture medium were collected on the second day of culturing. Activated HSCs were used as the experimental model, and serum without CTL was used as the blank control to compare the effects of serum components on HSCs. The fluid was changed every other day, cells were harvested on day 7 and total proteins or RNA was extracted for subsequent analysis of

Table I. Primer sequences used for reverse transcription-quantitative PCR.

Gene	Forward primer sequence (5'→3')	Reverse primer sequence (5'→3')
Colla1	CTGCCGATGTCGCTATCC	CCACAAGCGTGCTGTAGGT
α-SMA	TCCTGACCCTGAAGTATCCG	TCTCCAGAGTCCAGCACAAT
β-actin	CGTTGACATCCGTAAAGACC	GCTAGGAGCCAGGGCAGTA

Collagen I (*Colla1*) and α-smooth muscle actin (SMA) expression. To investigate the effects of CTL on the PI3K/Akt/mTOR pathway, activated HSC-T6 cells were treated at 4˚C for 2 h with 50 μg/ml 740Y-P, a PI3K agonist (Sigma-Aldrich; Merck KGaA), before CTL-infused serum treatment. Inactivated cells served as the controls; the cells were kept in a 5% CO_2 atmosphere at 37˚C in DMEM supplemented with 10% FBS. The fluid was changed every other day, cells were harvested on day 7, and total proteins or RNA was extracted for subsequent analysis of p-PI3K, PI3K, p-Akt, Akt, p-mTOR, mTOR, Collagen I and α-SMA expression, with 8 replicates per group (n=8).

Histopathological assay. Rat liver tissue specimens (1 cm^3) were fixed with 4% formaldehyde at room temperature for 24 h, embedded in paraffin, sliced into sections of 4 μm thickness, stained with hematoxylin (HE; 10 min) and eosin (1 min) (HE) and Masson stain (10 min) at room temperature, and observed under a light microscope.

Reverse transcription-quantitative PCR (RT-qPCR). Total RNA was extracted from rat liver tissues or HSCs with a mount of $1x10^5$ colony forming unit (cfu) using TRIzol® reagent (Thermo Fisher Scientific, Inc.). Following this, cDNA was synthesized from total RNA samples using the PrimeScript RT reagent Kit (Takara Bio, Inc.) for 15 min at 37˚C followed by 5 sec at 85˚C. qPCR was performed using SYBR Premix Ex Taq II (Takara Bio, Inc.) with an initial denaturation for 30 sec at 95˚C, followed by 40 cycles of amplification (95˚C for 5 sec and 60˚C for 34 sec), according to the manufacturer's protocol. The expression level of the target gene was normalized to that of β-actin and all RT-qPCR data were quantified using the $2^{-\Delta\Delta Cq}$ method (31) with the SLAN automated PCR Analysis System (8.2.2; Shanghai Hongshi Medical Technology Co., Ltd.), with the primer sequences listed in Table I.

Western blotting. A T-PER (for tissue) or M-PER (for cell) lysis buffer (Thermo Fisher Scientific, Inc.) containing a protease inhibitor mixture (Thermo Fisher Scientific, Inc.) was used to extract total proteins from liver tissues and cultured HSCs ($1x10^6$ cfu). The protein concentration was determined using a bicinchoninic acid-based protein assay kit (Thermo Fisher Scientific, Inc.). Each sample, containing 100 μg protein, was separated using 10% SDS-PAGE and transferred to a polyvinylidene fluoride membrane. The membrane was blocked with 5% skim milk for 1 h at room temperature under 50 x g centrifugation and incubated at 4˚C with primary antibodies overnight. Following incubation with secondary antibodies for 1 h at room temperature under 50 x g centrifugation, the membrane was observed with SuperSignal West Pico PLUS (Pierce; Thermo Fisher Scientific, Inc.) using enhanced chemiluminescence (TANON automated Chemiluminescence Imaging System 5200; Shanghai Tianneng Life Sciences Co., Ltd.; http://www.biotanon.com/). The detected protein levels were normalized to β-actin expression levels. The primary antibodies used were as follows: Anti-E-cadherin antibody (1:1,000; cat. no. ab231303; Abcam), anti- α-SMA antibody (1:1,000; cat. no. ab5694; Abcam), anti-SOX9 antibody (1:1,000; cat. no. ab185966; Abcam), anti-Collagen I antibody (1:1,000; cat. no. ab34710; Abcam), anti-phosphorylated (p-) Y607-PI3K antibody (1:1,000; cat. no. ab182651; Abcam), anti-p-T308 AKT (1:1,000; cat. no. ab38449; Abcam) and anti-p-S2491 mTOR (1:1,000; cat. no. ab137133; Abcam), anti-PI3K antibody (1:1,000; cat. no. ab191606; Abcam), anti-AKT antibody (1:2,000; cat. no. ab185633; Abcam), anti-mTOR antibody (1:10,000; cat. no. ab134903; Abcam) and anti-β-actin antibody (1:1,000; cat. no. ab8227; Abcam). The secondary antibodies used were as follows: Goat anti-mouse IgG HRP (1:5,000; cat. no. ab6789; Abcam) and goat anti-rabbit IgG HRP (1:5,000; cat. no. ab205718; Abcam).

ELISA. For aspartate transaminase (AST) and alanine transaminase (ALT) assays, using the Rat AST ELISA Kit (cat. no. ab263883; Abcam) and Rat ALT ELISA Kit (cat. no. ab234579; Abcam), were used according to the manufacturers' instructions. For the hydroxyproline assay, 100 mg liver tissue was homogenized at 4˚C for 1 min and treated with 1 ml 10N NaOH, and heated at 120˚C hermetically for 1 h. After which, 1 ml 10N HCl was added to neutralize NaOH, and the solution was centrifuged at 10,000 x g at 4˚C for 5 min. The supernatant was collected for measurement of hydroxyproline with a Hydroxyproline Assay kit (cat. no. ab222941; Abcam), according to the manufacturer's instructions. Total protein was used as an internal reference.

Statistical analysis. Data are presented as the mean ± SD and all experiments were repeated at least three times. The data were evaluated using one-way ANOVA, and statistical significance was determined using the Tukey's test. $P<0.05$ was considered to indicate a statistically significant difference. All statistical analyses were performed with GraphPad Prism (9.5; Dotmatics).

Results

CTL inhibits HF in vivo. To assess the effect of CTL in terms of inhibiting HF in rats, HE staining, Masson staining, biochemical tests and the detection of HF biomarkers were performed to determine the degree of HF. According to the HE staining results, hepatocytes in the control group were arranged neatly and exhibited normal morphology, and appeared to be radiating

from the central vein. No necrosis or inflammatory cell infiltration was observed. By contrast, the model group exhibited disordered hepatocyte alignment, extensive inflammatory cell infiltration (red arrows), and substantial fibrous tissue proliferation and bridging fibrosis around the veins. Compared with the model group, the CTL-treated groups showed varying degrees of improvement in the liver tissue structure and inflammatory response, with the CTL-H group demonstrating significant improvement (Fig. 1A). Masson staining revealed that the hepatic lobules in the control group were intact, with only a small amount of collagen fiber staining observed around the hepatic vein walls, indicative of the absence of collagen fiber proliferation. In the model group, the hepatic lobule structure was disrupted, and extensive and dense collagen fiber deposition (black arrows) that extended to form fibrous septa (yellow arrows) was observed around the hepatic veins and portal tracts. In comparison, the CTL-L and CTL-M groups showed thinning of the fibrous septa and reduced collagen fiber expression, while the CTL-H group exhibited complete regression of the fibrous septa and a reduction in collagen fibers (Fig. 1B). The results of both HE and Masson staining suggest that CTL can ameliorate CCl_4-induced liver injury and collagen deposition. In addition, AST and ALT levels were increased in the model group compared with the control group, whereas this increase was partially reduced on CTL administration (Fig. 1C and D). Moreover, the western blotting results showed that compared with the control group, the levels of the epithelial marker E-cadherin was significantly decreased in the model group, and the levels of the HF markers α-SMA and SOX9 were significantly increased. Following the administration of different concentrations of CTL, E-cadherin expression was found to be significantly increased, and α-SMA and SOX9 expression levels were significantly decreased, all of which occurred in a dose-dependent manner (Fig. 1E). The RT-qPCR and ELISA results showed that CTL could attenuate the increased expression levels of *Colla1*, *α-SMA* or hydroxyproline content induced by CCl_4 (Fig. 1F-H). The results indicated that CTL could inhibit HF *in vivo.*

CTL-infused serum inhibits activation of primary HSCs. To determine whether CTL-infused serum could inhibit HSC activation, primary HSCs were used. Observed under a light microscope, freshly isolated primary HSCs adhered to plastic cell culture flasks completely within 24 h, and after seven days of culture, they underwent a morphological change from a quiescent phenotype to an activated phenotype. The cells in model and blank serum group extended pseudopodia that fused and interconnected with each other and adopted a star-shaped morphology, with some cells already exhibiting fibroblast-like growth. By contrast, the CTL-infused serum was found to reduce the degree of fibrosis and alleviate the morphological changes in HSCs (Fig. 2A). The western blotting results showed that CTL significantly inhibited the expression of collagen I and α-SMA in activated HSCs in a dose-dependent manner (Fig. 2B). The RT-qPCR results concerning *Colla1* and *α-SMA* levels were consistent with the western blotting results (Fig. 2C and D). The results indicated that CTL could attenuate HSC activation.

Effect of CTL on the PI3K/Akt/mTOR pathways in rats with HF. The protein expression levels of p-PI3K, p-Akt and p-mTOR in the liver tissues of rats with HF were measured using western blot analysis. Compared with the control group, the expression levels of p-PI3K, p-Akt and p-mTOR were found to be significantly increased in the model group, which corroborated previous findings (32,33). CTL downregulated the expression levels of p-PI3K, p-Akt and p-mTOR in the control group in a dose-dependent manner (Fig. 3). These results suggest that CTL can inhibit the PI3K/Akt/mTOR pathway.

Effect of CTL-infused serum on the PI3K/Akt/mTOR pathways in HSC-T6 cells. To determine whether CTL-infused serum could inhibit PI3K/Akt/mTOR pathways in HSCs, the HSC-T6 cell line was used. In preliminary experiments, primary HSCs were found to be insensitive to the PI3K agonist 740Y-P. HSC-T6 cells were cultured *in vitro*, activated using TGF-β1 and CTL-infused serum was added to detect its inhibitory effect on the PI3K/Akt/mTOR pathway, using blank serum as a control. The results showed that TGF-β1 significantly increased the expression levels of p-PI3K, p-Akt and p-mTOR compared with the control. It was also observed that CTL-infused serum significantly decreased the expression levels of p-PI3K, p-Akt and p-mTOR. When the PI3K agonist 740Y-P was used to counteract the effect of CTL, the results showed that 740Y-P alone did not affect the PI3K/Akt/mTOR pathway but was able to block the effect of CTL in reducing p-PI3K, p-Akt and p-mTOR expression (Fig. 4A). It also blocked the expression-lowering effect of CTL on *Colla1* and *α-SMA* (Fig. 4B and C). These results indicate that CTL may directly act on PI3K and inhibit its phosphorylation, thus inhibiting the activation of HSCs.

Discussion

Stimulated by continuous pathogenic factors, HF can progress into hepatic cirrhosis or even hepatic carcinoma, both of which currently lack effective therapies (34). Numerous studies have explored various natural compounds such as *Acanthus ilicifolius* alkaloid A, berberine, caffeine, capsaicin, conophylline, evodiamine and ligustrazine in an attempt to find novel drugs to treat HF (35,36). Traditional Chinese or Mongolian medicine is a discipline based on practice and exploration. In general, the therapies used in these disciplines consist of combinations of various herbs (37). CTL is a common herb used in these medicinal paradigms to treat liver diseases, with a curative effect that has been well documented (38). In the present study, an animal model of HF was constructed through intraperitoneal injection of CCl_4 in rats, after which CTL was administered as an intervention. Through histopathological staining, Masson staining and the detection of HF markers, it was found that CTL could significantly relieve HF in a dose-dependent manner. In addition, CTL-infused serum was able to inhibit the activation of primary HSCs, and it was also demonstrated that CTL could inhibit the activation of the PI3K/Akt/mTOR pathway in both rats and HSC-T6, most likely by inhibiting the phosphorylation of PI3K.

The activation of HSCs is the initial and key step that induces HF (39). Upon liver injury or inflammation, quiescent HSCs undergo a phenotypic transformation termed activation (39). This process involves a complex interplay of various signaling pathways and molecular mechanisms (40). Initially, HSCs lose their

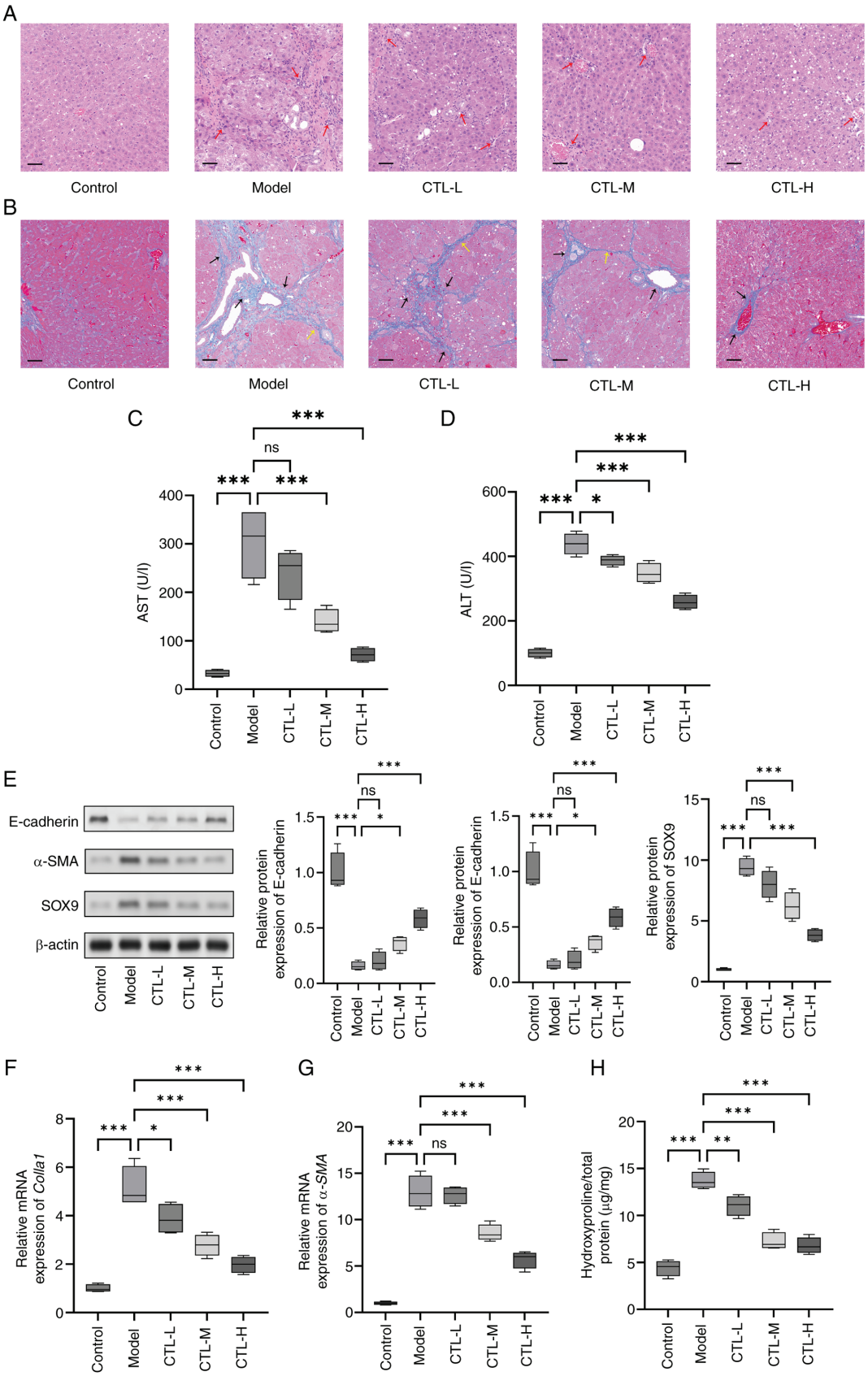

Figure 1. Inhibition of hepatic fibrosis by CTL under *in vivo* conditions. CCl_4-induced rat hepatic fibrosis models were treated with different concentrations of CTL (0.5, 1.0 and 1.5 g/kg/day). (A) Hematoxylin and eosin staining and (B) Masson staining showing that CTL can ameliorate CCl_4-induced liver histopathological injury. Red arrows represent extensive inflammatory cell infiltration, black arrows represent dense collagen fiber deposition and yellow arrows represent fibrous septa (magnification, x200; scale bar, 50 μm). (C) AST and (D) ALT levels measured by ELISA. (E) Protein expression levels of E-cadherin, α-SMA, and SOX-9, as measured using western blot analysis. (F) *Colla1* and (G) *α-SMA* mRNA levels as measured using reverse transcription-quantitative PCR. (H) Hydroxyproline level measured using ELISA. Results are presented as the mean ± SD (n=8), using one-way ANOVA. *P<0.05, **P<0.01 and ***P<0.001. ns, not significant; CTL, *Carthamus tinctorius L.*; HE, hematoxylin and eosin; AST, aspartate transaminase; ALT, alanine transaminase; α-SMA, α-smooth muscle actin; *Colla1*, collagen I, CTL-L, CTL low-dose group; CTL-M, CTL medium-dose group; CTL-H, CTL high-dose group.

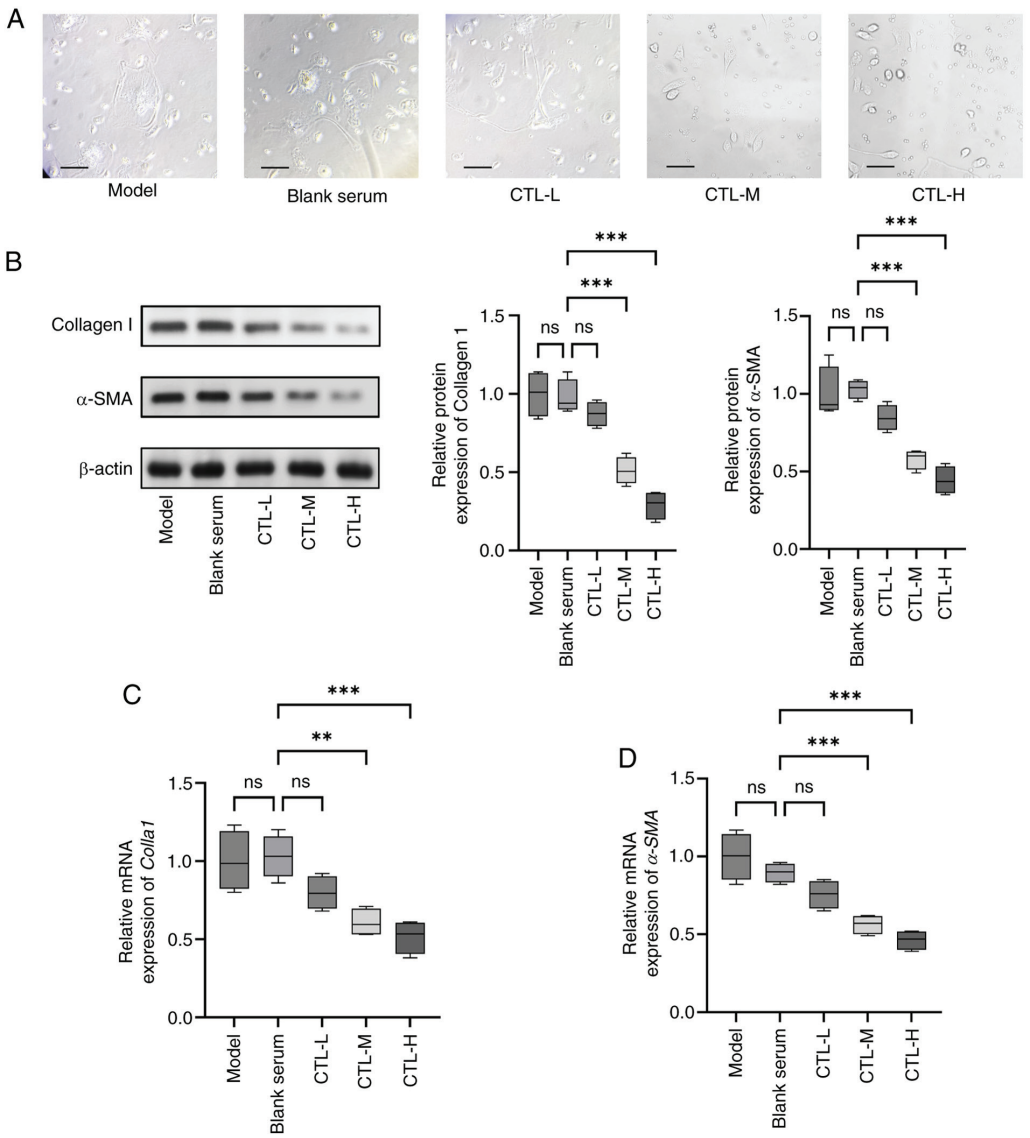

Figure 2. Inhibition of activation of primary HSCs by CTL-infused serum. Primary HSCs were treated with different concentrations of CTL-infused serum (0.5, 1.0 and 1.5 g/kg/day). (A) Morphological changes in primary HSCs (magnification, x400; scale bar, 50 μm). (B) Protein expression levels of collagen I and α-SMA, as measured using western blot analysis. (C) *Colla1* and (D) *α-SMA* mRNA levels as measured using reverse transcription-quantitative PCR. Results are presented as the mean ± SD (n=8), using one-way ANOVA. **P<0.01 and ***P<0.001. ns, not significant; CTL, *Carthamus tinctorius L.*; α-SMA, α-smooth muscle actin; HSCs, hepatic stellate cells; *Colla1*, collagen I, CTL-L, CTL low-dose group; CTL-M, CTL medium-dose group; CTL-H, CTL high-dose group.

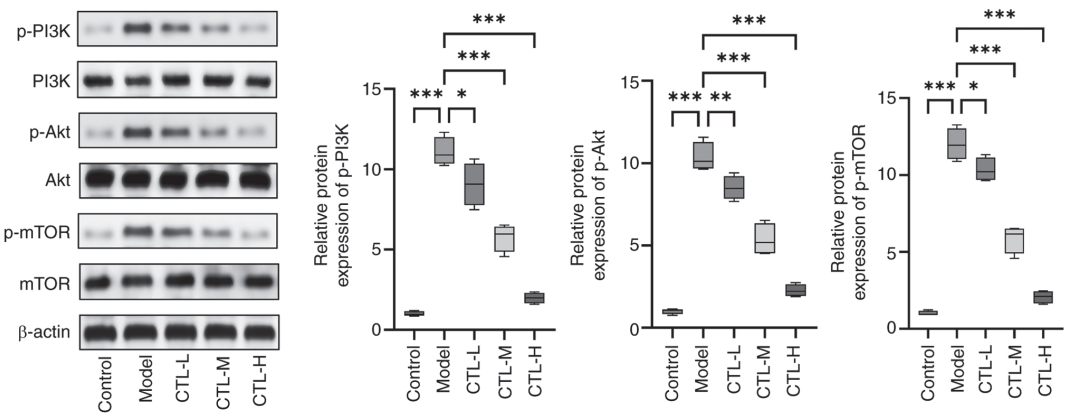

Figure 3. Effect of CTL on the PI3K/Akt/mTOR pathway in rats with hepatic fibrosis. CCl_4-induced rat hepatic fibrosis models were treated with different concentrations of CTL (0.5, 1.0 and 1.5 g/kg/day). Protein expression levels of p-PI3K, PI3K, p-Akt, Akt, p-mTOR and mTOR were measured using western blot analysis. Results are presented as the mean ± SD (n=8), using one-way ANOVA. *P<0.05, **P<0.01 and ***P<0.001. CTL, *Carthamus tinctorius L*; p-, phosphorylated.

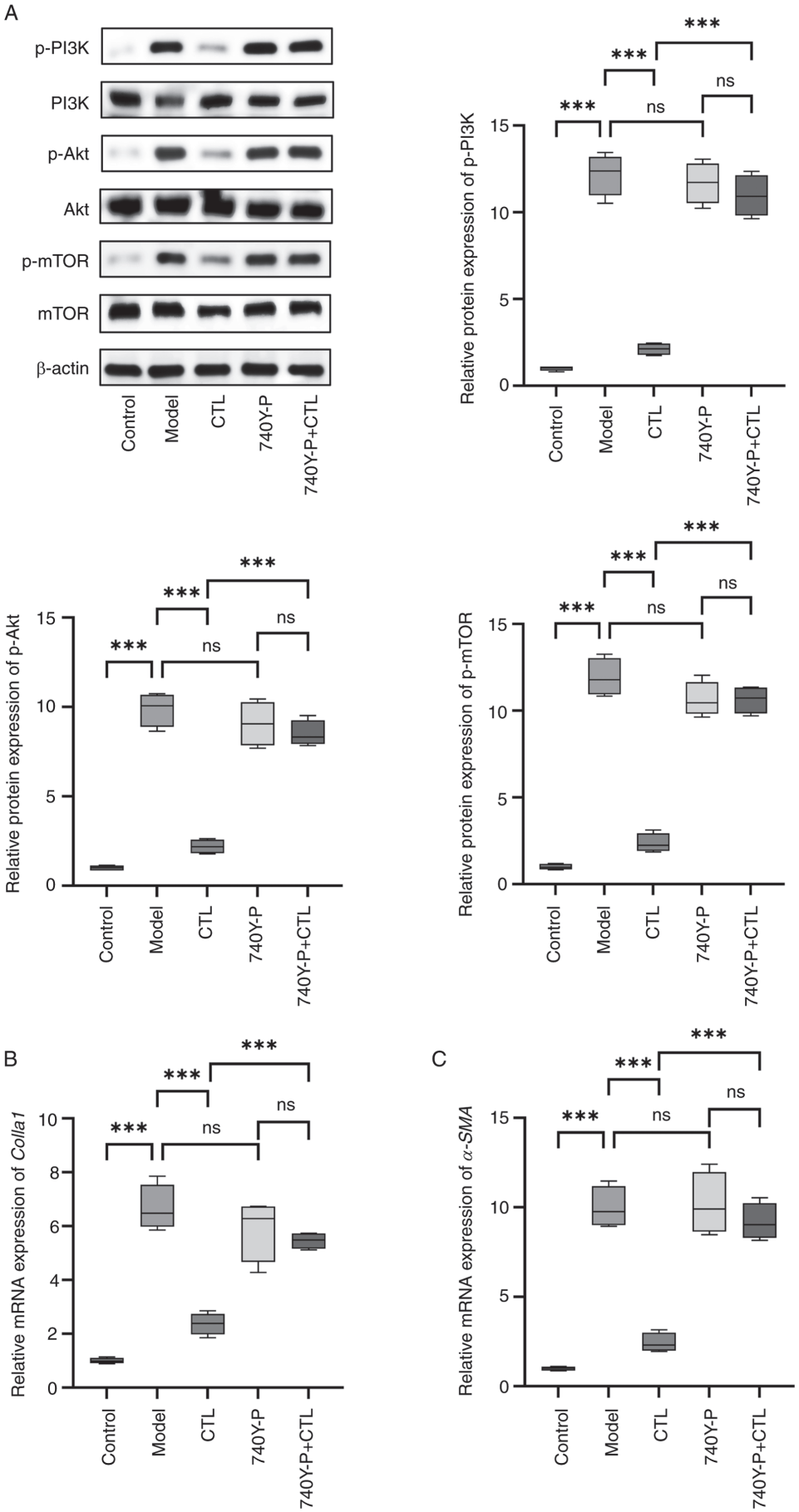

Figure 4. Effect of CTL on the PI3K/Akt/mTOR pathways in HSC-T6 cells. (A) Protein expression levels of p-PI3K, PI3K, p-Akt, Akt, p-mTOR and mTOR, as measured using western blot analysis. (B) *Colla1* and (C) *α-SMA* mRNA levels measured using reverse transcription-quantitative PCR Results are presented as the mean ± SD (n=8), using one-way ANOVA. ***P<0.001. ns, not significant; CTL, *Carthamus tinctorius L.*; p-, phosphorylated.

characteristic lipid droplets and transition into an activated state characterized by increased proliferation, contractility and synthesis of ECM components (41). Activation of HSCs is orchestrated by a multitude of factors including cytokines, growth factors and oxidative stress, ultimately leading to the deposition of excessive ECM proteins (42). As a major component of the ECM, collagen I is significantly upregulated during HF and serves as a key marker of fibrogenesis (43). Accumulation of collagen I disrupts the normal liver architecture and contributes to the formation of fibrotic scar tissue (44). Moreover, collagen I promotes HSC activation by inducing profibrogenic signaling pathways such as TGF-β/Smad and PI3K/Akt (45). Expression of α-SMA is a hallmark of activated HSCs and is closely associated with their contractile phenotype (46). α-SMA-positive myofibroblasts are responsible for the increased contractility observed in fibrotic liver tissue (47). Activation of HSCs leads to the upregulation of α-SMA expression, facilitating their contractile function and promoting ECM remodeling (48). Hydroxyproline is a non-proteinogenic amino acid predominantly found in collagen proteins Elevated levels of hydroxyproline serve as a reliable biomarker for increased collagen turnover and fibrogenesis in the liver. During HSC activation, there is a notable increase in hydroxyproline content, reflecting enhanced collagen synthesis and deposition. Measurement of hydroxyproline levels provides valuable insights into the extent of liver fibrosis and the efficacy of antifibrotic therapies (49).

The results of the present study showed that CTL can downregulate the expression of collagen I and α-SMA and reduce the production of hydroxyproline. Moreover, CTL also inhibited morphological changes in primary HSCs, implying that the inhibitory effect of CTL on HF may be related to its inhibition of HSC activation. Activated HSCs lead to over-deposition of ECM components, as well as the release of significant amounts of cytokines and inflammatory factors that eventually cause HF (50). Collagen I is the main component of the ECM, while hydroxyproline is an important element of collagen, and α-SMA is an important biomarker of HSC activation (7).

The PI3K/Akt pathway is the key mechanism affecting HF, and the inhibition of PI3K/Akt is considered to be an important target for HF intervention (51). Researchers have found that exosomes, miRNA, lncRNA, and natural drugs such as isovitexin, salvianolic acid A, germacrone and leonurine can inhibit HF by inhibiting the PI3K/Akt pathway (14,15,52,53). A previous study found that lncRNA GAS5 or LOC102551149 could act as molecular sponges to absorb miR-23a and inhibit the activation of PI3K/Akt/mTOR (32). Studies have shown that monomeric compounds from natural plants can inhibit the activation of the PI3K/Akt pathway in activated HSCs or animals with HF. For example, one study showed that forsythiaside A could downregulate the NOX4-ROS signaling pathway in HSCs, improve oxidation imbalance, inhibit the PI3K/Akt pathway and inhibit HSC activation (54). In addition, Galangin has been shown to promote apoptosis of HSCs by inhibiting the PI3K/Akt and Wnt/β-catenin pathways and increasing the Bax/Bcl-2 ratio (55). Furthermore, Inonotsuoxide B can inhibit HSC activation and proliferation by inhibiting both PI3K/Akt and ERK1/2 (56). However, these studies are still in the early stages, so few drugs have been developed based on these findings that are currently available for clinical use.

In the present study, CTL was found to effectively inhibit the activation of the PI3K/Akt pathway, and this effect was blocked using the PI3K activator 740Y-P. CTL is a natural plant-based medicine that contains a variety of biologically active ingredients. For example, carthamin yellow can reduce ROS release and inflammation to protect the heart against ischemia and reperfusion (57). In addition, Hydroxysafflor yellow A can regulate inflammation via the inhibition of PI3K in macrophages to reduce atherosclerosis (58). Quercetin can reduce p-PI3K levels to alleviate chronic renal failure (59). Anhydrosafflor yellow B protects against injuries caused by cerebral ischemia and reperfusion by attenuating oxidative stress and apoptosis via the silent information regulator 1 signaling pathway (60). Apigenin can inhibit the PI3K/Akt/mTOR pathway to induce apoptosis and autophagy in hepatocellular carcinoma cells (61). Furthermore, scutellarein can downregulate PI3K/Akt/NF-κB signaling to inhibit HepG2 cell proliferation and metastasis (62).

In the *in vivo* cellular experiments in the present study, cells were treated with CTL-infused serum. In general, it is hypothesized that if the components in the plants are not absorbed into the blood, it is difficult for them to reach the liver and exert their effects. The components of CTL extracts, CTL-infused serum and blank serum were tested, and 207 components in the extract of CTL and 220 components in the CTL-infuse were identified. Subsequently, components that were also detected in the blank serum were excluded, and 75 components remained in the CTL-infused serum. Of the 75 components identified in the CTL-infused serum, 20 were shared with the CTL extracts. The remaining 55 components may be produced by the metabolism of CTL, but they may also originate from the serum components of different animals (data not shown). However, the active ingredients from the 75 components detected was not identified. The present study results revealed that blank serum had no effect on the expression of collagen I and α-SMA, whereas CTL-infused serum could downregulate the expression of collagen I and α-SMA. These results are largely consistent with the results of the present study. Additionally, the present study aimed to ensure the reliability of the results through multiple repetitions of experiments (n=8). Therefore, the limitation of the present study is that monomeric compounds with anti-HF activity have not yet been confirmed. Despite this, further experiments using monomeric compounds are required to validate their anti-HF effect.

CTL at present is regarded as a herbal medicine with a high safety profile and is therefore, not highly regulated (63). The present study preliminarily demonstrated the anti-HF effect of CTL and provided a theoretical basis for the development of CTL as a therapy for HF treatment.

Acknowledgements

Not applicable.

Funding

The study was funded by The National Natural Science Foundation of China (grant nos. 82160794 and 82160703); Major Project of Natural Science Foundation of Inner Mongolia Autonomous Region (grant nos. 2021ZD14 and 2023ZD15); Nature Science Foundation of Inner Mongolia Autonomous Region (grant nos. 2020MS08046 and 2020MS08106);

Science and Technology Planning Project of Inner Mongolia Autonomous Region (grant nos. 2020GG0138); Program for Young Talents of Science and Technology in Universities of Inner Mongolia Autonomous Region (grant no. NJYT23114); Inner Mongolia Autonomous Region 'Prairie excellence' Project; Western Light Young Scholars Program of the Chinese Academy of Sciences; 'Prairie Talents' Leading Talent Project in Inner Mongolia Autonomous Region; Key Program of Inner Mongolia Medical University (grant no. YKD2022ZD013); Health Science and Technology Program of Inner Mongolia Health Commission (grant nos. 202201238 and 202202158); PhD Initial Funding Project of the Affiliated Hospital of Inner Mongolia Medical University (grant no. NYFY BS 202120); Inner Mongolia Medical University 'Youth Pioneering' Team Alliance (grant no. QNLC-2020064); Inner Mongolia Medical University Mongolian Medicine 'First-class Discipline' Construction Project (grant no. myxylxk2022019); and 2021 'Qihuang' scholar supporting project.

Availability of data and materials

The data generated in the present study may be requested from the corresponding author.

Authors' contributions

LB and LW conceived and designed the research; ZD, HG, LL, YZ and LW performed the experiments and analyzed the data; and LB drafted manuscript. ZD and HG confirm the authenticity of all the raw data. All authors read and approved the final version of the manuscript.

Ethics approval and consent to participate

All experiments in the present study were approved by The Ethics Committee of Inner Mongolia Medical University (Hohhot, China; approval no. YKD202201124).

Patient consent for publication

Not applicable.

Competing interests

The authors declare that they have no competing interests.

References

1. Boursier J, Roux M, Costentin C, Chaigneau J, Fournier-Poizat C, Trylesinski A, Canivet CM, Michalak S, Le Bail B, Paradis V, *et al*: Practical diagnosis of cirrhosis in non-alcoholic fatty liver disease using currently available non-invasive fibrosis tests. Nat Commun 14: 5219, 2023.
2. Roehlen N, Saviano A, El Saghire H, Crouchet E, Nehme Z, Del Zompo F, Jühling F, Oudot MA, Durand SC, Duong FHT, *et al*: A monoclonal antibody targeting nonjunctional claudin-1 inhibits fibrosis in patient-derived models by modulating cell plasticity. Sci Transl Med 14: eabj4221, 2022.
3. Ajmera V, Cepin S, Tesfai K, Hofflich H, Cadman K, Lopez S, Madamba E, Bettencourt R, Richards L, Behling C, *et al*: A prospective study on the prevalence of NAFLD, advanced fibrosis, cirrhosis and hepatocellular carcinoma in people with type 2 diabetes. J Hepatol 78: 471-478, 2023.
4. Luo P, Liu D, Zhang Q, Yang F, Wong YK, Xia F, Zhang J, Chen J, Tian Y, Yang C, *et al*: Celastrol induces ferroptosis in activated HSCs to ameliorate hepatic fibrosis via targeting peroxiredoxins and HO-1. Acta Pharm Sin B 12: 2300-2314, 2022.
5. Li Z, Wang F, Li Y, Wang X, Lu Q, Wang D, Qi C, Li C, Li Z, Lian B, *et al*: Combined anti-hepatocellular carcinoma therapy inhibit drug-resistance and metastasis via targeting 'substance P-hepatic stellate cells-hepatocellular carcinoma' axis. Biomaterials 276: 121003, 2021.
6. Dat NQ, Thuy LTT, Hieu VN, Hai H, Hoang DV, Thi Thanh Hai N, Thuy TTV, Komiya T, Rombouts K, Dong MP, *et al*: Hexa histidine-tagged recombinant human cytoglobin deactivates hepatic stellate cells and inhibits liver fibrosis by scavenging reactive oxygen species. Hepatology 73: 2527-2545, 2021.
7. Myojin Y, Hikita H, Sugiyama M, Sasaki Y, Fukumoto K, Sakane S, Makino Y, Takemura N, Yamada R, Shigekawa M, *et al*: Hepatic stellate cells in hepatocellular carcinoma promote tumor growth via growth differentiation factor 15 production. Gastroenterology 160: 1741-1754.e16, 2021.
8. Li WX, Chen X, Yang Y, Huang HM, Li HD, Huang C, Meng XM and Li J: Hesperitin derivative-11 suppress hepatic stellate cell activation and proliferation by targeting PTEN/AKT pathway. Toxicology 381: 75-86, 2017.
9. Parsons CJ, Takashima M and Rippe RA: Molecular mechanisms of hepatic fibrogenesis. J Gastroenterol Hepatol 22 (Suppl 1): S79-S84, 2007.
10. Shamsan E, Almezgagi M, Gamah M, Khan N, Qasem A, Chuanchuan L and Haining F: The role of PI3k/AKT signaling pathway in attenuating liver fibrosis: A comprehensive review. Front Med (Lausanne) 11: 1389329, 2024.
11. Lin X, Wei Y, Li Y, Xiong Y, Fang B, Li C, Huang Q, Huang R and Wei J: Tormentic acid ameliorates hepatic fibrosis in vivo by inhibiting glycerophospholipids metabolism and PI3K/Akt/mTOR and NF-κB pathways: Based on transcriptomics and metabolomics. Front Pharmacol 13: 801982, 2022.
12. Meng YX, Zhao R and Huo LJ: Interleukin-22 alleviates alcohol-associated hepatic fibrosis, inhibits autophagy, and suppresses the PI3K/AKT/mTOR pathway in mice. Alcohol Clin Exp Res (Hoboken) 47: 448-458, 2023.
13. Wang X, Liu H, Wang Y, Wang P, Yi Y, Lin Y and Li X: Novel protein C6ORF120 promotes liver fibrosis by activating hepatic stellate cells through the PI3K/Akt/mTOR pathway. J Gastroenterol Hepatol 39: 1422-1430, 2024.
14. Wang R, Song F, Li S, Wu B, Gu Y and Yuan Y: Salvianolic acid A attenuates CCl_4-induced liver fibrosis by regulating the PI3K/AKT/mTOR, Bcl-2/Bax and caspase-3/cleaved caspase-3 signaling pathways. Drug Des Devel Ther 13: 1889-1900, 2019.
15. Ji D, Zhao Q, Qin Y, Tong H, Wang Q, Yu M, Mao C, Lu T, Qiu J and Jiang C: Germacrone improves liver fibrosis by regulating the PI3K/AKT/mTOR signalling pathway. Cell Biol Int 45: 1866-1875, 2021.
16. Zhang LL, Tian K, Tang ZH, Chen XJ, Bian ZX, Wang YT and Lu JJ: Phytochemistry and pharmacology of *Carthamus tinctorius L*. Am J Chin Med 44: 197-226, 2016.
17. Delshad E, Yousefi M, Sasannezhad P, Rakhshandeh H and Ayati Z: Medical uses of *Carthamus tinctorius L*. (safflower): A comprehensive review from traditional medicine to modern medicine. Electron Physician 10: 6672-6681, 2018.
18. Okuyama H, Yamada K, Miyazawa D, Yasui Y and Ohara N: Dietary lipids impacts on healthy ageing. Lipids 42: 821-825, 2007.
19. Suzuki K, Tsubaki S, Fujita M, Koyama N, Takahashi M and Takazawa K: Effects of safflower seed extract on arterial stiffness. Vasc Health Risk Manag 6: 1007-1014, 2010.
20. Liang Y and Wang L: *Carthamus tinctorius L*.: A natural neuroprotective source for anti-Alzheimer's disease drugs. J Ethnopharmacol 298: 115656, 2022.
21. Ao H, Feng W and Peng C: Hydroxysafflor yellow A: A promising therapeutic agent for a broad spectrum of diseases. Evid Based Complement Alternat Med 2018: 8259280, 2018.
22. Bai J, Wang X, Du S, Wang P, Wang Y, Quan L and Xie Y: Study on the protective effects of danshen-honghua herb pair (DHHP) on myocardial ischaemia/reperfusion injury (MIRI) and potential mechanisms based on apoptosis and mitochondria. Pharm Biol 59: 335-346, 2021.
23. Du SB, Zhou HH, Wang PF, Wang XP, Xue ZP, Li J, Gao S, Li N, Bai JQ and Xie LH: Modulation effects of danshen-honghua herb pair on gut microbiota of acute myocardial ischemia model rat. FEMS Microbiol Lett 369: fnac036, 2022.

24. Wan H, Yang Y, Li Z, Cheng L, Ding Z, Wan H, Yang J and Zhou H: Compatibility of ingredients of Danshen (Radix Salviae Miltiorrhizae) and Honghua (Flos Carthami) and their protective effects on cerebral ischemia-reperfusion injury in rats. Exp Ther Med 22: 849, 2021.
25. Liu Y, Zhou B and Ding X: Informatic study of cada prescription for the treatment of liver disease. TCM Pharmacol Clin 39: 104-110, 2023.
26. Meng X, Zhou B and Liu Y: Data mining of the 'Bashaga' class (Qumai) prescription prescription and its action mechanism analysis for the treatment of liver disease. Chin Mod TCM 25: 1266-1279, 2023.
27. Uriga, Wang Y and Nao M: Progress in experimental research on Mongolian drug therapy for liver injury. World Sci Technol-Modern Tradit Chin Med 22: 416-422, 2020.
28. Yang T, Liang S and Zhou B: Progress in the treatment of liver fibrosis. Chin Ethnic Folk Med 28: 68-71, 2019.
29. Chang LL, Li C, Li ZL, Wei ZL, Jia XB, Pang ST, An YQ, Gu JF and Feng L: *Carthamus tinctorius L*: Extract ameliorates cerebral ischemia-reperfusion injury in rats by regulating matrix metalloproteinases and apoptosis. Indian J Pharmacol 52: 108-116, 2020.
30. Greenfield EA: Sampling and preparation of mouse and rat serum. Cold Spring Harb Protoc 2017: pdb.prot100271, 2017.
31. Livak KJ and Schmittgen TD: Analysis of relative gene expression data using real-time quantitative PCR and the 2(-Delta Delta C(T)) method. Methods 25: 402-408, 2001.
32. Dong Z, Li S, Si L, Ma R, Bao L and Bo A: Identification lncRNA LOC102551149/miR-23a-5p pathway in hepatic fibrosis. Eur J Clin Invest 50: e13243, 2020.
33. Dong Z, Li S, Wang X, Si L, Ma R, Bao L and Bo A: lncRNA GAS5 restrains CCl_4-induced hepatic fibrosis by targeting miR-23a through the PTEN/PI3K/Akt signaling pathway. Am J Physiol Gastrointest Liver Physiol 316: G539-G550, 2019.
34. Ali MH, Talha M and Hussain SAS: The role of hepatic stellate cells and the Gas6/Axl axis in liver fibrosis and hepatocellular carcinoma. J Clin Exp Hepatol 14: 101400, 2024.
35. Shan L, Liu Z, Ci L, Shuai C, Lv X and Li J: Research progress on the anti-hepatic fibrosis action and mechanism of natural products. Int Immunopharmacol 75: 105765, 2019.
36. Shan L, Wang F, Zhai D, Meng X, Liu J and Lv X: New drugs for hepatic fibrosis. Front Pharmacol 13: 874408, 2022.
37. Li D, Tao L, Chen Z, Cai W and Shen W: Treatment of peripheral facial paralysis after COVID-19 infection with traditional chinese medicine therapies: A case report. Cureus 16: e57047, 2024.
38. Xi S, Yue L, Shi M, Peng Y, Xu Y, Wang X, Li Q, Kang Z, Li H and Wang Y: The effects of taoren-honghua herb pair on pathological microvessel and angiogenesis-associated signaling pathway in mice model of CCl4-induced chronic liver disease. Evid Based Complement Alternat Med 2016: 2974256, 2016.
39. Wan S, Liu X, Sun R, Liu H, Jiang J and Wu B: Activated hepatic stellate cell-derived Bmp-1 induces liver fibrosis via mediating hepatocyte epithelial-mesenchymal transition. Cell Death Dis 15: 41, 2024.
40. Hwang CH, Jang E and Lee JH: Pharmacological benefits and underlying mechanisms of Salvia miltiorrhiza against molecular pathology of various liver diseases: A review. Am J Chin Med 51: 1675-1709, 2023.
41. Tuohetahuntila M, Molenaar MR, Spee B, Brouwers JF, Wubbolts R, Houweling M, Yan C, Du H, VanderVen BC, Vaandrager AB and Helms JB: Lysosome-mediated degradation of a distinct pool of lipid droplets during hepatic stellate cell activation. J Biol Chem 292: 12436-12448, 2017.
42. Sharma A, Verma AK, Kofron M, Kudira R, Miethke A, Wu T, Wang J and Gandhi CR: Lipopolysaccharide reverses hepatic stellate cell activation through modulation of cMyb, small mothers against decapentaplegic, and CCAAT/enhancer-binding protein C/EBP transcription factors. Hepatology 72: 1800-1818, 2020.
43. Li R, Zhang J, Liu Q, Tang Q, Jia Q, Xiong Y, He J and Li Y: CREKA-modified liposomes target activated hepatic stellate cells to alleviate liver fibrosis by inhibiting collagen synthesis and angiogenesis. Acta Biomater 168: 484-496, 2023.
44. Yin L, Zhang Y, Shi H, Feng Y, Zhang Z and Zhang L: Proteomic profiling of hepatic stellate cells in alcohol liver fibrosis reveals proteins involved in collagen production. Alcohol 86: 81-91, 2020.
45. Zhang M, Wu Z, Salas SS, Aguilar MM, Trillos-Almanza MC, Buist-Homan M and Moshage H: Arginase 1 expression is increased during hepatic stellate cell activation and facilitates collagen synthesis. J Cell Biochem 124: 808-817, 2023.
46. Ezquerro S, Tuero C, Becerril S, Valentí V, Moncada R, Landecho MF, Catalán V, Gómez-Ambrosi J, Mocha F, Silva C, *et al*: Antagonic effect of ghrelin and LEAP-2 on hepatic stellate cell activation and liver fibrosis in obesity-associated nonalcoholic fatty liver disease. Eur J Endocrinol 188: 564-577, 2023.
47. Jokl E, Llewellyn J, Simpson K, Adegboye O, Pritchett J, Zeef L, Donaldson I, Athwal VS, Purssell H, Street O, *et al*: Circadian disruption primes myofibroblasts for accelerated activation as a mechanism underpinning fibrotic progression in non-alcoholic fatty liver disease. Cells 12: 1582, 2023.
48. Hussein KH, Park KM, Yu L, Kwak HH and Woo HM: Decellularized hepatic extracellular matrix hydrogel attenuates hepatic stellate cell activation and liver fibrosis. Mater Sci Eng C Mater Biol Appl 116: 111160, 2020.
49. Bissoondial TL, Han Y, Mullan S, Pabla AK, Spahn K, Shi S, Zheng L, Zhou P, Jiang K, Prakash N, *et al*: Liver biopsy hydroxyproline content is a diagnostic for hepatocellular carcinoma in murine models of nonalcoholic steatohepatitis. Diagnostics (Basel) 10: 784, 2020.
50. Zhou L, Liang Q, Li Y, Cao Y, Li J, Yang J, Liu J, Bi J and Liu Y: Collagenase-I decorated co-delivery micelles potentiate extracellular matrix degradation and hepatic stellate cell targeting for liver fibrosis therapy. Acta Biomater 152: 235-254, 2022.
51. Lopez-Sanchez I, Dunkel Y, Roh YS, Mittal Y, De Minicis S, Muranyi A, Singh S, Shanmugam K, Aroonsakool N, Murray F, *et al*: GIV/Girdin is a central hub for profibrogenic signalling networks during liver fibrosis. Nat Commun 5: 4451, 2014.
52. Huang Y, Luo W, Chen S, Su H, Zhu W, Wei Y, Qiu Y, Long Y, Shi Y and Wei J: Isovitexin alleviates hepatic fibrosis by regulating miR-21-mediated PI3K/Akt signaling and glutathione metabolic pathway: Based on transcriptomics and metabolomics. Phytomedicine 121: 155117, 2023.
53. Yu Y, Zhou S, Wang Y, Di S, Wang Y, Huang X and Chen Y: Leonurine alleviates acetaminophen-induced acute liver injury by regulating the PI3K/AKT signaling pathway in mice. Int Immunopharmacol 120: 110375, 2023.
54. Zhou M, Zhao X, Liao L, Deng Y, Liu M, Wang J, Xue X and Li Y: Forsythiaside A regulates activation of hepatic stellate cells by inhibiting NOX4-dependent ROS. Oxid Med Cell Longev 2022: 9938392, 2022.
55. Xiong Y, Lu H and Xu H: Galangin reverses hepatic fibrosis by inducing HSCs apoptosis via the PI3K/Akt, Bax/Bcl-2, and Wnt/β-catenin pathway in LX-2 cells. Biol Pharm Bull 43: 1634-1642, 2020.
56. Jin J, Yang H, Hu L, Wang Y, Wu W, Hu C, Wu K, Wu Z, Cheng W and Huang Y: Inonotsuoxide B suppresses hepatic stellate cell activation and proliferation via the PI3K/AKT and ERK1/2 pathway. Exp Ther Med 23: 417, 2022.
57. Lu QY, Ma JQ, Duan YY, Sun Y, Yu S, Li B and Zhang GM: Carthamin yellow protects the heart against ischemia/reperfusion injury with reduced reactive oxygen species release and inflammatory response. J Cardiovasc Pharmacol 74: 228-234, 2019.
58. Feng X, Du M, Li S, Zhang Y, Ding J, Wang J, Wang Y and Liu P: Hydroxysafflor yellow A regulates lymphangiogenesis and inflammation via the inhibition of PI3K on regulating AKT/mTOR and NF-κB pathway in macrophages to reduce atherosclerosis in ApoE-/- mice. Phytomedicine 112: 154684, 2023.
59. Tu H, Ma D, Luo Y, Tang S, Li Y, Chen G, Wang L, Hou Z, Shen C, Lu H, *et al*: Quercetin alleviates chronic renal failure by targeting the PI3k/Akt pathway. Bioengineered 12: 6538-6558, 2021.
60. Fangma Y, Zhou H, Shao C, Yu L, Yang J, Wan H and He Y: Hydroxysafflor yellow A and anhydrosafflor yellow B protect against cerebral ischemia/reperfusion injury by attenuating oxidative stress and apoptosis via the silent information regulator 1 signaling pathway. Front Pharmacol 12: 739864, 2021.
61. Yang J, Pi C and Wang G: Inhibition of PI3K/Akt/mTOR pathway by apigenin induces apoptosis and autophagy in hepatocellular carcinoma cells. Biomed Pharmacother 103: 699-707, 2018.
62. Ha SE, Kim SM, Vetrivel P, Kim HH, Bhosale PB, Heo JD, Lee HJ and Kim GS: Inhibition of cell proliferation and metastasis by scutellarein regulating PI3K/Akt/NF-κB signaling through PTEN activation in hepatocellular carcinoma. Int J Mol Sci 22: 8841, 2021.
63. Shuang R, Qirigeer, Wurihan, Bai M, Laxinamujila and Han X: Toxicity of *Carthamus tinctorius* L. Water Extract. World Trad Chin Med 18: 979-982, 2023 (In Chinese).